In situ correction of the spherical aberration in a double-toroidal electron analyzer

Xiao-Jing Liu,[1,2,a)] Christophe Nicolas,[2] and Catalin Miron[2,3,b)]
[1]*School of Physics and Nuclear Energy Engineering, Beihang University, Beijing 100191, China*
[2]*Synchrotron SOLEIL, L'Orme des Merisiers, Saint-Aubin, BP 48, F-91192 Gif-sur-Yvette Cedex, France*
[3]*Extreme Light Infrastructure Nuclear Physics (ELI-NP), 'Horia Hulubei' National Institute for Physics and Nuclear Engineering, 30 Reactorului Street, RO-077125 Măgurele, Judet Ilfov, Romania*

(Received 15 December 2016; accepted 20 January 2017; published online 13 February 2017)

In an energy-dispersive electron spectrometer, the electrons with the same kinetic energy but different polar angles fly along different paths and impinge upon the detector at different locations. This behavior materializes the spherical aberration of the electron optics, which deteriorates the focussing quality on the detector, and thus the energy resolution of the instrument. Here, we demonstrate that, in general, the electron time of flight changes monotonically as a function of the polar angle. Combining the impact position on the detector and the time of flight of electrons, the spherical aberration can be corrected and the energy resolution can be significantly improved, 1.5× in the case of our double toroidal analyser. This correction method has a general applicability and can be of interest to experimentalists willing to push further the performances of their electron spectrometers when the time of flight is available. *Published by AIP Publishing.* [http://dx.doi.org/10.1063/1.4975379]

I. INTRODUCTION

Electron spectroscopy plays a key role in the study of materials.[1–4] Different kinds of electron spectrometers have been developed to fit the specific needs of various research fields[5–8] and used together with a variety of ionization sources enabling ionization energies from a few eV to several keV.[9] On the one hand, the electron kinetic energies encode rich information about electronic structure, via the measured binding energies and chemical shifts,[10] as well as about the potential energy surfaces[11] of the relevant electronic states. On the other hand, the line profiles and the electron angular distributions provide information on various types of dynamics occurring in the electronic states.[12–14]

Most often, electron spectra are measured using electrostatic, energy-dispersive spectrometers, which consist of an energy-dispersive analyzer coupled to a transfer lens and a detector. The performance of an electron spectrometer is determined by the electron kinetic energy resolution achieved, the transmission efficiency of lens, and the parallel detection capabilities. To improve the kinetic energy resolution, the aberrations and defects introduced by the electrostatic transfer lens need to be corrected. There are still ongoing efforts to reduce the spherical aberration, coma, and astigmatism.[15–17] Although the commercial electron spectrometers, mainly based on hemispherical electrostatic analyzers, dominate the field of electron spectroscopy,[18] innovative homemade electron spectrometers are still developed by individual groups to meet their own needs. Double toroidal analyzer (DTA)[19–21] represents such a good example; our double toroidal analyzer (DTA) was developed some 20 years ago[22,23] and its lens table was accomplished only very recently.[24]

In order to improve the performance of this spectrometer, the spherical aberrations need to be reduced as much as possible. A simple method could be to decrease the acceptance angle of the electrons. However, this would reduce the efficiency of the instrument, which is undesired especially in coincidence experiments.

In this article, we show that if the time of flight of the electrons is measured, this additional information enables us to correct the spherical aberration. As the result, the energy resolution of our DTA is improved by about a factor of 1.5.

II. INSTRUMENTAL SETUP

All details about the high transmission efficiency DTA can be found in Refs. 22–24. A schematic drawing of the DTA is shown in Fig. 1. In brief, it consists of two sets of toroidal analyzers mounted in series, each one consisting of two deflectors. They are configured to ensure that the output focal surface is planar, thus enabling simultaneous recording of the energy and of the azimuthal angles of the electrons using a planar position sensitive detector. L0 is a grounded collimator, which defines the accepted polar angle interval, whereas L1, L2, L3, and L4 form a four-element lens that transfers and focuses, for a given pass energy, E_p, the electrons with the kinetic energy E_k from the source volume onto the entrance slit of the DTA. Electrons are then energy dispersed between the two pairs of deflecting plates of the DTA and focused on a planar position sensitive detector. The distance between the inner and the outer deflecting plates is 12 mm, corresponding to a gross etendue—the total width of the electron kinetic energy window in which the electrons can be analyzed simultaneously—of about 14% of the pass energy. The whole system has an axial symmetry

a)Electronic mail: xjliu@buaa.edu.cn
b)Electronic mail: catalin.p.miron@gmail.com

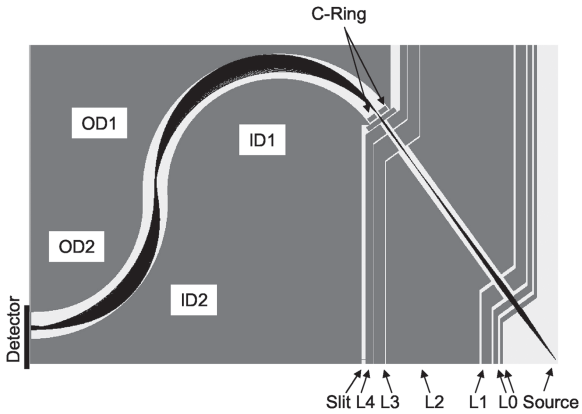

FIG. 1. The double toroidal analyzer with its transfer lens. L0 is the grounded collimator. L1, L2, L3, and L4 form the transfer lens. The correction rings (C-Ring) are installed behind the entrance slit to compensate the fringe fields. ID1, ID2, OD1, and OD2 are the four deflecting plates of the analyzer. The black lines are simulated trajectories of electrons with a kinetic energy of 494 eV and a DTA pass energy of 50 eV.

and the source volume is located on the symmetry axis (see Fig. 1). The L0 collimator geometry allows to simultaneously collect electrons emitted with polar angles α in the range $54 \pm 3°$ and azimuthal angles from 0° to 360°, those ranges corresponding to 0.53 sr. This acceptance is about one order of magnitude higher than the one achieved by the state-of-the-art commercial hemispherical electron energy analyzers equipped with wide angle lens electron optics and makes the DTA very attractive for multicoincidence experiments. As an example, electron trajectories simulated with $(E_k, E_p) = (494\ \text{eV}, 50\ \text{eV})$ are shown in Fig. 1.

All voltages applied to the analyzer and electrostatic lens electrodes are remotely controlled using commercial power supplies from VG Scienta AB. The accuracy of the voltages is better than 0.1 V. A DLD40 position sensitive detector[25] based on a delay-line anode from RoentDek Handels GmbH[26] is used for the electron detection.

III. RESULTS AND DISCUSSION

For a toroidal analyzer with the mid-radius R_0 operated at the pass energy E_p, when an electron beam with a pencil-angle $\Delta\alpha$ is accepted, the energy resolution ΔE is given by[27]

$$\frac{\Delta E}{E_p} = \frac{\omega}{DR_0} + \kappa(\Delta\alpha)^2. \quad (1)$$

Here ω is the width of entrance and exit slits, and D and κ are two geometric parameters. A similar argument works for DTA as well. So, the energy resolution always gets worse as the pencil-angle $\Delta\alpha$ increases.

The time of flight of the electron depends on both the kinetic energy and the polar angle. While the dependence of electron time of flight on the kinetic energy was already taken into account in the previous data analysis of (e, 2e) experiments in order to improve the signal to noise ratio,[19,20] its dependence on the polar angle was not yet discussed in details. The simulations (see Fig. 2(a)) indicate that the electron time of flight varies within the pencil angle. This behavior can be understood as follows: On the one hand, compared

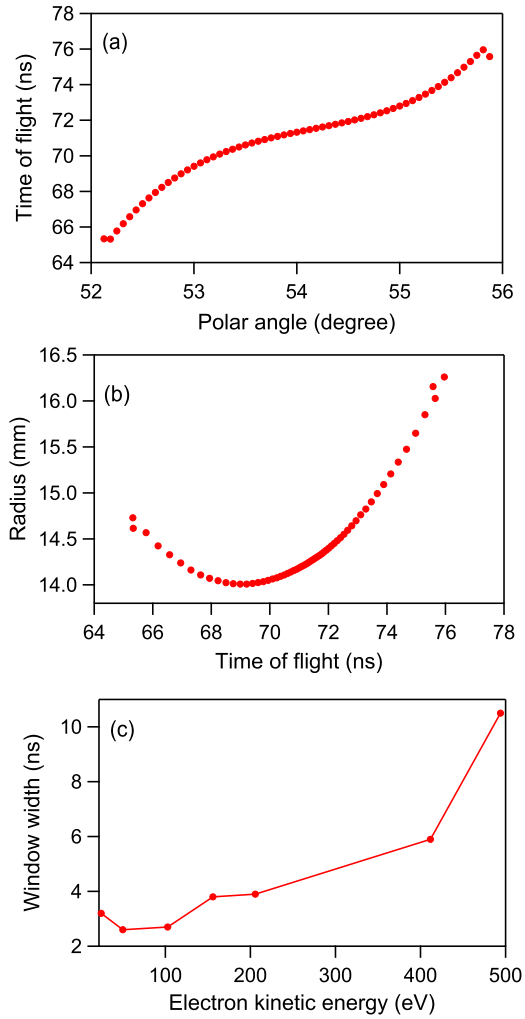

FIG. 2. Results of numerical simulations: (a) The electron time of flight as a function of the polar angle; (b) the radius of the electron image as a function of the time of flight at $(E_k, E_p) = (494\ \text{eV}, 50\ \text{eV})$; (c) the width of the time of flight window as a function of the electron kinetic energy at $E_p = 50$ eV.

with the electrons with nominal polar angle of 54°, the electrons with larger polar angles are decelerated during the first half of their trajectories and then accelerated during the second half within each toroid. Thus they have a lower averaged speed and a longer path (see Ref. 22), so their time of flight is getting longer. On the other hand, the electrons with smaller polar angle will then correspondingly have a shorter time of flight. This means that the time of flight will change monotonically as a function of the polar angle of the electron. As a result, the electron time of flight provides a measurement of the polar angle and can be used to correct the spherical aberration.

The results of simulations using Simion 3D software are shown in Fig. 2. In Fig. 2(a), the simulations show that for a typical set of parameters $(E_k, E_p) = (494\ \text{eV}, 50\ \text{eV})$, the time of flight increases monotonically by about 10 ns as the polar angle increases, which confirms our arguments above. We also checked that, with different initial kinetic energies, the electrons fully cover the etendue of the DTA and their time of flight varies by about 3 ns, which is much smaller than 10 ns here. We further plot the radius of the electron image against

the time of flight in Fig. 2(b). It can approximately be represented by a quadratic polynomial function, which is similar to the typical behavior of spherical aberration shown in Eq. (1). Finally, we ran simulations at several electron kinetic energies, as shown in Fig. 2(c). It can be seen that the width of the time of flight window increases as the electron kinetic energy increases. This can be understood as a result of Liouville's theorem: as the electron kinetic energy increases, the pencil angle of electron at the entrance of the DTA gets larger, thus the spherical aberration gets larger and the electron time of flight window gets also broader.

To confirm the result of the simulations, we measured the photoelectrons from Kr $3d_{3/2,5/2}$ orbitals at a photon energy of 587 eV in the single bunch mode at the PLEIADES beamline at synchrotron SOLEIL. We recorded each individual event, including the bunch marker, with a multi-channel time-to-digital converter (TDC) card.[26] Since the polar angle cannot be directly measured, only the electron image radius as a function of the time of flight is given in Fig. 3(a). The measured

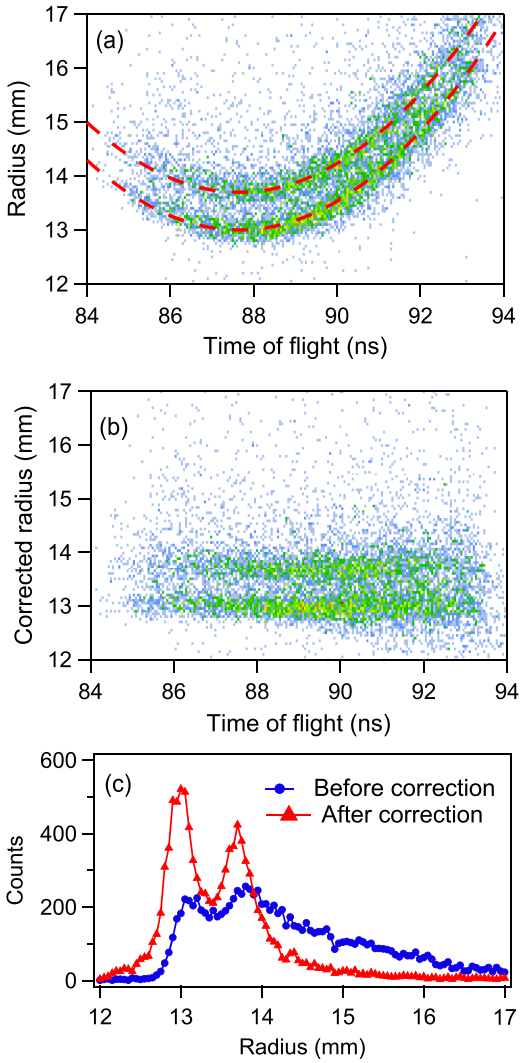

FIG. 3. The measured dependence of radius of the electron image on the time of flight (a) before and (b) after correction, respectively. The electrons are ionized from Kr $3d_{3/2,5/2}$ orbitals, respectively. The two dashed lines in (a) represent the function used for correction. The spectrum plotted against the electron image radius before/after the correction is shown in (c). The resolution is improved greatly by incorporating the correction.

dependencies agree well with the simulated one in Fig. 2(b), and an empirical formula can be used to correct the measured radius,

$$r_c = r + c(t - t_0)^2, \tag{2}$$

where r and r_c are the radius before and after correction, respectively. c and t_0 are fitting coefficients.

The corrected radius becomes independent of time of flight of the electron, as shown in Fig. 3(b). For convenience of the comparison, the spectra plotted against the electron image radius before/after the correction are plotted in Fig. 3(c). It can be seen that the position resolution is improved by about 1.5×. After appropriate scaling, the energy resolution is improved by the same amount.

IV. SUMMARY AND CONCLUSIONS

In conclusion, by recording the time of flight of the electrons in addition to their impact position on a position sensitive detector, we demonstrated a method to correct the spherical aberration of a double-toroidal analyzer. This is a new step further in the experimental efforts to improve the energy resolution of electron spectrometers. Very recently, a new upsurge appeared in investigating the time-dependent phenomena on surfaces or in superconductors using time-resolved and angularly resolved photoelectron spectroscopy.[28,29] Unfortunately, the electron time of flight is not recorded in most cases. Our proposed method offers a simple and robust algorithm to sensibly improve the experimental resolution of such measurements.

ACKNOWLEDGMENTS

Data collection was performed at the PLEIADES beamline at the SOLEIL Synchrotron, France (in-house beamtime allocation). We are grateful to E. Robert for technical assistance and to the SOLEIL staff for stable operation of the equipment and the storage ring during the experiments. X.J.L. gratefully acknowledges the financial support by the National Natural Science Foundation of China (11574020) and Project of Thousand Youth Talents in China.

[1] F. J. Himpsel, Adv. Phys. **32**, 1 (1983).
[2] O. Bjorneholm, G. Ohrwall, and M. Tchaplyguine, Nucl. Instrum. Methods Phys. Res., Sect. A **601**, 161 (2009).
[3] C. Miron and P. Morin, "High-resolution photoionization, photoelectron and coincidence spectroscopy," in *Handbook of High-Resolution Spectroscopy* (John Wiley and Sons, Inc., 2011), pp. 1655–1689.
[4] C. Miron and M. Patanen, Adv. Mater. **26**, 7911 (2014).
[5] H. Siegbahn and L. Karlsson, in *Hundbuch der Physik*, edited by W. Mehlhorn (Springer, Berlin, 1982), Vol. 31.
[6] J. Eland, *Photoelectron Spectroscopy: An Introduction to Ultraviolet Photoelectron Spectroscopy in the Gas Phase* (Butterworths, 1984).
[7] *Applications of Synchrotron Radiation*, edited by W. Eberhardt (Springer-Verlag, Berlin, 1994).
[8] G. Ohrwall, P. Karlsson, M. Wirde, M. Lundqvist, P. Andersson, D. Ceolin, B. Wannberg, T. Kachel, H. Durr, W. Eberhardt, and S. Svensson, J. Electron Spectrosc. Relat. Phenom. **183**, 125 (2011).
[9] K. Siegbahn, Rev. Mod. Phys. **54**, 709 (1982).
[10] K. Siegbahn, C. Nordling, G. Johansson, J. Hedman, P. F. Heden, K. Hamrin, U. Gelius, T. Bergmark, L. O. Werme, R. Manne, and Y. Baer, *ESCA Applied to Free Molecules* (North-Holland Publishing Co., Amsterdam, London, 1969).

[11] C. Miron, C. Nicolas, O. Travnikova, P. Morin, Y. Sun, F. Gel'mukhanov, N. Kosugi, and V. Kimberg, Nat. Phys. **8**, 135 (2012).
[12] J. Cooper and R. N. Zare, J. Chem. Phys. **48**, 942 (1968).
[13] P. Morin and I. Nenner, Phys. Rev. Lett. **56**, 1913 (1986).
[14] K. Ueda, M. Kitajima, A. De Fanis, T. Furuta, H. Shindo, H. Tanaka, K. Okada, R. Feifel, S. L. Sorensen, H. Yoshida, and Y. Senba, Phys. Rev. Lett. **90**, 233006 (2003).
[15] E. Harting and F. H. Read, *Electrostatic Lenses* (Elsevier, Amsterdam, 1976).
[16] P. Baltzer, B. Wannberg, and M. C. Göthe, Rev. Sci. Instrum. **62**, 643 (1991).
[17] J. Moore, C. Davis, and M. Coplan, *Building Scientific Apparatus*, 3rd ed. (Cambridge University, MA, 2003).
[18] N. Mårtensson, P. Baltzer, P. A. Brühwiler, J.-O. Forsell, A. Nilsson, A. Stenborg, and B. Wannberg, J. Electron Spectrosc. Relat. Phenom. **70**, 117 (1994).
[19] R. C. G. Leckey and J. D. Riley, Appl. Surf. Sci. **22-23**, 196 (1985).
[20] J. Lower, R. Panajotovic, S. Bellm, and E. Weigold, Rev. Sci. Instrum. **78**, 111301 (2007).
[21] P. Zhang, C. Xu, Y. Tang, and X. Chen, J. Electron Spectrosc. Relat. Phenom. **193**, 39 (2014).
[22] C. Miron, M. Simon, N. Leclercq, and P. Morin, Rev. Sci. Instrum. **68**, 3728 (1997).
[23] K. Le Guen, D. Céolin, R. Guillemin, C. Miron, N. Leclercq, M. Bougeard, M. Simon, P. Morin, A. Mocellin, F. Burmeister, A. Naves de Brito, and S. L. Sorensen, Rev. Sci. Instrum. **73**, 3885 (2002).
[24] X.-J. Liu, C. Nicolas, and C. Miron, Rev. Sci. Instrum. **84**, 033105 (2013).
[25] O. Jagutzki, V. Mergel, K. Ullmann-Pfleger, L. Spielberger, U. Spillmann, R. Dörner, and H. Schmidt-Böcking, Nucl. Instrum. Methods Phys. Res., Sect. A **477**, 244 (2002).
[26] See http://www.Roentdek.com for RoentDek Handels GmbH, 2012.
[27] T. J. Reddish, G. Richmond, G. W. Bagley, J. P. Wightman, and S. Cvejanovic, Rev. Sci. Instrum. **68**, 2685 (1997).
[28] C. L. Smallwood, J. P. Hinton, C. Jozwiak, W. Zhang, J. D. Koralek, H. Eisaki, D.-H. Lee, J. Orenstein, and A. Lanzara, Science **336**, 1137 (2012).
[29] D. N. Basov, M. M. Fogler, A. Lanzara, F. Wang, and Y. Zhang, Rev. Mod. Phys. **86**, 959 (2014).